Effects of Elevated Intraocular Pressure on Retinal Ganglion Cell Density and Expression and Interaction of Retinal Aquaporin 9 and Monocarboxylate Transporters

Murai, Yusuke ; Mori, Sotaro ; Okuda, Mina ; Kusuhara, Sentaro ; Kurimoto, Takuji ; Nakamura, Makoto

(Citation)
Ophthalmic Research,66(1):1222-1229

(Issue Date)
2023-08-30

(Resource Type)
journal article

(Version)
Version of Record

(URL)
https://hdl.handle.net/20.500.14094/0100483298

Ophthalmic Research

Research Article

Ophthalmic Res 2023;66:1222–1229
DOI: 10.1159/000533497

Received: February 10, 2023
Accepted: August 4, 2023
Published online: August 30, 2023

Effects of Elevated Intraocular Pressure on Retinal Ganglion Cell Density and Expression and Interaction of Retinal Aquaporin 9 and Monocarboxylate Transporters

Yusuke Murai Sotaro Mori Mina Okuda Sentaro Kusuhara
Takuji Kurimoto Makoto Nakamura

Division of Ophthalmology, Department of Surgery, Kobe University Graduate School of Medicine, Kobe, Japan

Keywords
Astrocyte-to-neuron lactate shuttle · Monocarboxylate transporter · Aquaporin 9 · Retinal ganglion cell · Glaucoma

Abstract
Introduction: Astrocyte-to-neuron lactate shuttle (ANLS) plays an important role in the energy metabolism of neurons, including retinal ganglion cells (RGCs). Aquaporin 9 (AQP9), which is an aquaglyceroporin that can transport lactate, may be involved in ANLS together with monocarboxylate transporters (MCTs) to maintain RGC function and survival. This study aimed to investigate the impact of elevated intraocular pressure (IOP) on AQP9-MCT interaction and RGC survival. ***Methods:*** IOP was elevated in *Aqp9* knock-out (KO) mice and wild-type (WT) littermates by anterior chamber microbead injection. RGC density was measured by TUBB3 immunostaining on retinal flat mounts. Immunolabeling, immunoblot, and immunoprecipitation were conducted to identify and quantitate expressions of AQP9, MCT1, MCT2, and MCT4 in whole retinas and ganglion cell layer (GCL). ***Results:*** *Aqp9* KO and WT mice had similar RGC density at baseline. Microbead injection increased cumulative IOP by approximately 32% up to 4 weeks, resulting in RGC density loss of 42% and 34% in WT and *Aqp9* KO mice, respectively, with no statistical difference. In the retina of WT mice, elevated IOP decreased the amount of AQP9, MCT1, and MCT2 protein and changed the AQP9 immunoreactivity and reduced MCT1 and MCT2 immunoreactivities in GCL. Meanwhile, it decreased MCT1 and increased MCT2 that interact with AQP9, without affecting MCT4 expression. *Aqp9* gene deletion increased baseline MCT2 expression in the GCL and counteracted IOP elevation regarding MCT1 and MCT2 expressions. ***Conclusion:*** The compensatory upregulation of MCT1 and MCT2 with *Aqp9* gene deletion and ocular hypertension may reflect the need to maintain lactate transport in the retina for RGC survival.

Introduction

Glaucoma is an optic neuropathy wherein retinal ganglion cells (RGCs) and their axon bundles, the optic nerve, degenerate and drop out, thereby impairing visual function and quality of life, with elevated intraocular pressure (IOP) as a major risk factor [1]. Evidence has been accumulating that astrocyte-to-neuron lactate shuttle (ANLS) plays an important role in maintaining neuronal metabolism, function, and survival [2, 3]. Astrocytes in ANLS are thought to take up glucose from blood vessels, convert it to lactate, and release the lactate

karger@karger.com
www.karger.com/ore

Correspondence to:
Makoto Nakamura, manakamu@med.kobe-u.ac.jp

toward neurons. Lactate taken up by neurons is converted to pyruvate and then metabolized in the tricarboxylic acid cycle to produce adenosine triphosphate.

Aquaporin 9 (AQP9) belongs to the aquaglyceroporins and is permeable not only to water but also to monocarboxylates including lactate [4]. AQP9 is expressed in catecholaminergic amacrine cells [5], RGCs [6–8], and astrocytes in the retina. RGC expression of AQP9 is decreased in rodent eyes with elevated IOP [6], optic nerve crush (ONC) [3] or transection [7], and glaucomatous human eyes [8]. Furthermore, we previously demonstrated that L-lactate requires AQP9 expression to maintain RGC survival in culture [9]. These lines of evidence suggest that AQP9 is involved as a lactate transporter in ANLS in the inner retina.

Other key players in ANLS are members of the proton-linked monocarboxylate transporter (MCT) family [2, 3, 10, 11]. In the brain, endothelial cells and glia are known to express MCT1 and MCT4, and neurons express MCT2. MCT1 and MCT4 are presumed to mainly release lactate and MCT2 to take up lactate [2, 3, 10, 11]. We have recently reported that AQP9 and MCT1, MCT2, and MCT4 are co-expressed in RGCs, and ONC reduces their expression and dissociates their protein-protein interactions, which has an adverse effect on RGC survival and function [3]. However, the impact of elevated IOP on the interaction between AQP9 and MCTs in the retina and its association with RGC death are unknown. This study aimed to determine how elevated IOP affects retinal AQP9 and MCT expression and their interaction and RGC survival in the retina by inducing ocular hypertension in wild-type (WT) and *Aqp9* knock-out (KO) mice by microbead (MB) injection into the anterior chamber.

Materials and Methods

Animals

The *Aqp9* KO (*Aqp9*–/–) mice were a gift from Professor Søren Nielsen of the Department of Biomedicine of Aarhus University, Denmark [12, 13]. These mice are C57BL/6J background mice with targeted gene disruption of *Aqp9* and exhibit normal development, fertility, and appearance [3, 12]. The experiments used 20–25-week-old male *Aqp9* KO mice and their WT littermates (*Aqp9*+/+) (body weight, 25–35 g). A total of 64 mice were housed at the Kobe University animal breeding facility under a 12 h light/12 h dark period (room temperature, 24 ± 2°C) with free access to food and water.

MB Injection into Anterior Chamber

The mouse model of chronic ocular hypertension by MB injection into the anterior chamber was partially modified from previous reports [14–16]. Mice were anesthetized with intraperitoneal administration of a ketamine (100 mg/kg) and xylazine (10 mg/kg) mixture, and the pupil of the left eye was pharmacologically dilated with 0.5% tropicamide and 0.5% phenylephrine hydrochloride mixed ophthalmic solution (Santen Pharmaceutical Co., Osaka, Japan). The cornea was punctured with a 32-gauge needle. Then, a hand-made beveled glass capillary (1.0/0.75 mm outer diameter/inner diameter without filament, Novato, USA) connected to a Hamilton syringe was used to inject 6 μL of magnetic MBs (8 μm diameter, 6×10^6 beads/mL in phosphate buffered saline [PBS]; COMPEL™ Magnetic, COOH modified; Bangs Laboratories, Inc., USA), followed by the injection of 4 μL of air bubbles (AB). The beads were pulled into the anterior chamber angle with a hand-held neodymium magnet to occlude the trabecular meshwork. The right eye was left untreated. Another group of control mice was injected with 6 μL of PBS (pH, 7.5; Cell Science & Technology Institute Inc., Sendai, Japan) and 4 μL of AB into the anterior chamber of the left eye. The mice were allowed to recover on a heating pad. Each group comprised 16 mice.

IOP in awake mice was measured at the indicated time points for 4 weeks using a rebound tonometer (TonoLab; TioLat, Finland) [3, 16]. IOP was measured six times in each session, and internal software was used to eliminate the highest and lowest readings and average the remaining values. Cumulative IOP (mm Hg/day) was calculated by multiplying the mean IOP value by the number of days after MB injection [17].

RGC Density Measurement

Four mice per each group were sacrificed at 2 weeks or 4 weeks after treatments and perfused with 4% paraformaldehyde. Immunolabeling of retinal flat mounts with an anti-tubulin β3 (TUBB3) antibody (BioLegend, USA) was performed to visualize RGCs [3]. Briefly, explanted retinas were incubated for 2 h at room temperature in a blocking solution of 5% bovine serum albumin (BSA) in PBS containing 0.1% Triton X-100 (PBS-T) followed by incubation in PBS-T with Alexa Fluor (AF) 488 conjugated anti-TUBB3 antibody (1: 500) overnight at 4°C. Then, the retinas were washed with PBS-T and mounted on glass slides. An observer (T.K.), masked to mouse processing conditions, counted the number of TUBB3-positive cells at two points (1 mm and 2 mm from the optic disc) in each quadrant (temporal, nasal, inferior, and superior) retinal region captured by fluorescence microscopy (Biozero BZ-8000, Keyence, Japan) using a 40× objective lens, that is, 0.145 mm^2 per field of view, for a total of 8 fields per retina. Cell density was calculated from these images using NIH ImageJ software. The error coefficient was less than 0.05, which confirms the adequate sampling rate [18].

Retinal Thin Section Immunostaining

Frozen sections of the retina (8-μm thick; 4 mice per group at 4 weeks after treatments) were collected on glass slides and fixed in 4% paraformaldehyde for 10 min. The sections were incubated overnight at 4°C with the appropriate concentration of primary antibody after blocking with PBS-T containing 5% BSA. Following extensive washes, they were incubated with secondary antibodies for 1 h at room temperature. Then, they were washed and mounted in coverslips. The primary antibodies used included chicken anti-AQP9 (1:200, Abcam, Japan), rabbit anti-MCT1, MCT2, and MCT4 (1:500, 1:200, and 1:200, respectively; Bioss, USA). The

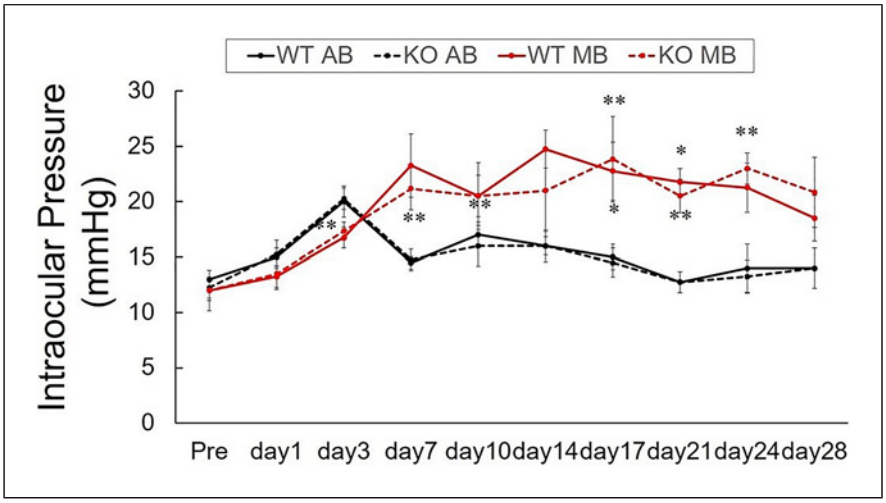

Fig. 1. Time course of changes in the IOP of 4 groups of mice. n = 16 per group between Pre and day 14. Thereafter, n = 16 each in WT AB and KO AB and n = 12 each in WT MB and KO MB. *and **are significant differences after Bonferroni's correction compared to Pre in the WT MB and KO MB mice, respectively. See text for specific values at each time point. WT, wild-type; KO, *Aqp9* knock-out; AB, air bubble; MB, microbeads; Pre, pre-treatment.

secondary antibodies used included AF488-anti-chicken goat IgG (1:500, Themo Fisher Scientific KK, Japan) and AF594-anti-rabbit goat IgG (1:500, Thermo Fisher Scientific KK).

Immunoprecipitation

Immunoprecipitation was performed using the Dynabeads Protein A Immunoprecipitation Kit (Invitrogen, Carlsbad, CA, USA) to determine the interaction between AQP9 and MCTs, following the manufacturer's instructions [3]. Briefly, retinas from 3 eyes per group at 4 weeks after treatments were homogenized in lysate buffer (0.1 M of sucrose, 0.1 M ethylenediaminetetraacetic acid [EDTA], 20 mM Tris-HCl pH 7.5, 2.5 mM sodium pyrophosphate, and one tablet of cOmplete tablets EDTA-free Protease Inhibitor Cocktail [Sigma-Aldrich, USA]) and homogenized by sonication. After centrifugation, the collected supernatant was incubated in 1% sodium dodecyl sulfate for 30 min. Samples were then centrifuged at 23,000 *g* for 30 min. The protein concentration of the supernatant was quantified using NanoDrop Lite (Thermo Fisher Scientific KK). Retinal lysate samples containing 800 μg of total protein were incubated with 2 μL of rabbit anti-AQP9 (1:40; Abcam) for 10 min at room temperature, followed by incubation with Dynabeads Protein A for 10 min. The beads were collected by placing the tube on a magnet. Elution of Dynabeads-antibody-antigen complex was used for further immunoblot analysis.

Immunoblot Analysis

Retinal proteins (60 μg) from whole-cell homogenates (4 eyes per group at 4 weeks after treatments) or eluates of the above-mentioned Dynabeads-antibody-antigen complexes were incubated in Laemmli loading buffer containing 20 mM dithiothreitol at 95°C for 5 min, followed by sodium dodecyl sulfate-polyacrylamide gel electrophoresis (Thermo Fisher Scientific KK) and subsequent transfer on a polyvinylidene difluoride membrane (GE Healthcare Life Sciences, UK). The membrane was blocked with 5% BSA in Tris-buffered saline containing 0.1% Tween 20 (TBS-T) for 1 h at room temperature, then incubated overnight at 4°C with primary antibodies in TBS-T, including rabbit anti-AQP9 (1:5,000, Abcam), MCT1, MCT2, and MCT4 (1:1,000, see above), and β-actin (1:200, Abcam). Then, the membrane was incubated with horseradish peroxidase-conjugated anti-rabbit IgG (1:2,000) at room temperature for 1 h. ECL reagents (GE Healthcare Life Sciences) was used for chemiluminescence detection. The relative ratio of signal to β-actin expression was quantified for total protein immunoblots, while the relative ratio of signal to WT control was quantified for immunoprecipitate immunoblots, using a LAS-3000 Mini digital imaging system (Fujifilm, Tokyo, Japan).

Statistical Analysis

Data are reported as mean ± standard deviation. Statistical analyses were performed using MedCalc software version 20.210 (MedCalc Software, Belgium). Statistical comparisons were made by one-way or repeated measures analysis of variance (ANOVA) when comparing three or more groups, and by unpaired t test when comparing two groups. The Tukey-Kramer test was used for post hoc analysis. A p value of <0.05 was considered statistically significant. Bonferroni-corrected p values were used for repeated IOP measurements in the same individuals.

Results

IOP Changes

Figure 1 illustrates baseline and post-injection IOP changes among 4 treatment groups. Baseline IOP in the WT AB, KO AB, WT MB, and KO MB mice were 13.0 ± 0.8, 12.3 ± 1.0, 12.0 ± 1.8, and 12.0 ± 0.9 mm Hg, respectively, with no significant difference among the groups (p = 0. 56). The WT MB group had significantly higher IOP at 17 (p value with Bonferroni's correction [Pc] = 0.009) and 21 days (Pc = 0.012), while the KO MB group had significantly higher IOP at 3 (Pc = 0.0095), 7 (Pc = 0.007), 10 (Pc = 0.006), 17 (Pc = 0.043), 21 (Pc = 0.003), and 24 (Pc = 0.001) days. No significant difference was found in IOP compared to baseline in the WT AB and KO AB mice. Hence, the cumulative IOP at 4 weeks

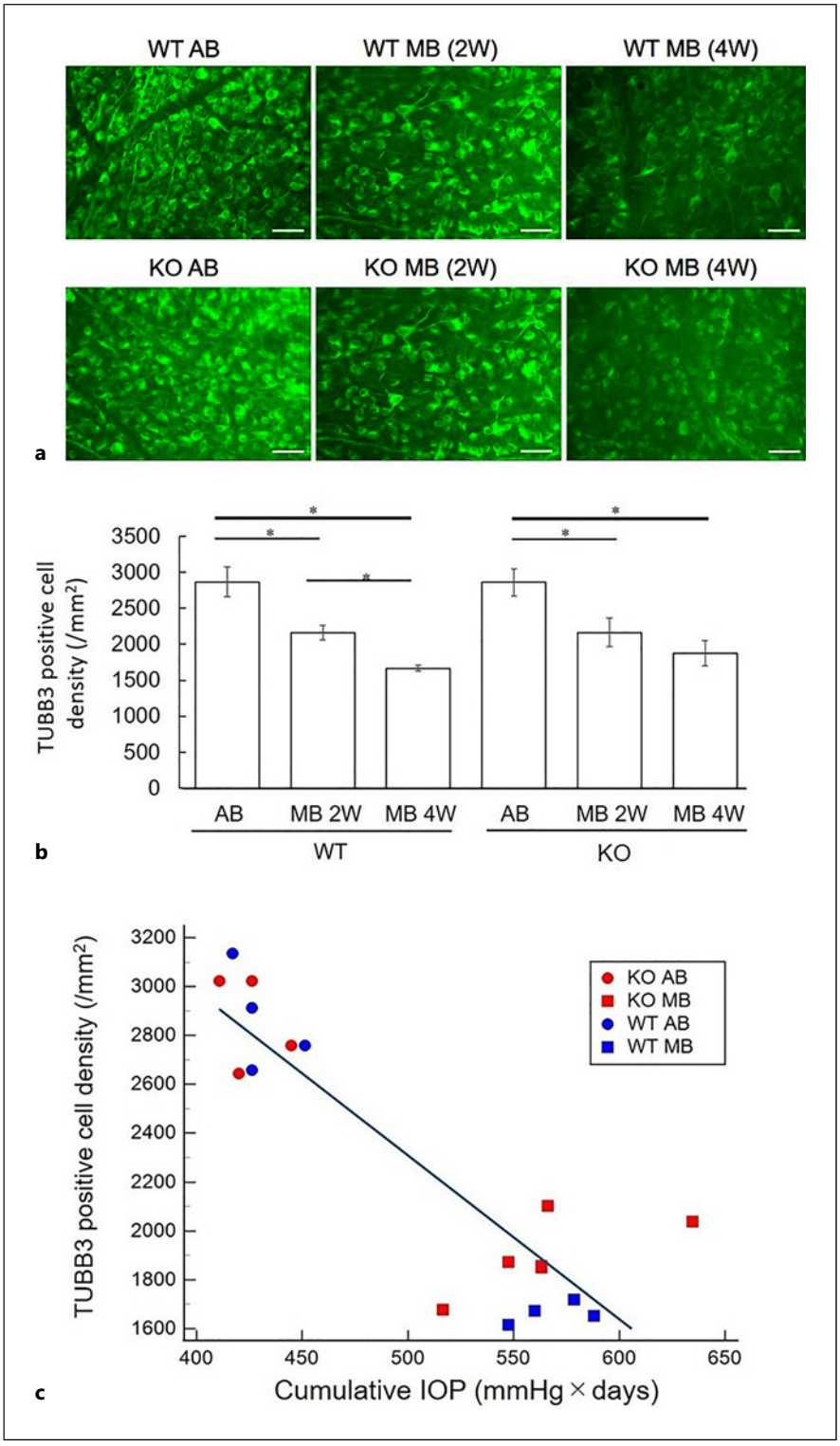

Fig. 2. Changes in RGC density of 4 groups of mice. **a** Representative TUBB3 immunolabeling images. Scale bar, 50 μm. **b** Data quantification. $n = 4$ per group. WT AB and KO AB were mice sacrificed at 4 weeks after treatment. *ANOVA, $p < 0.001$; Tukey-Kramer test, $p < 0.05$. **c** Scatter plots of TUBB3-positive cell density against cumulative IOP. All data were obtained from mice sacrificed at 4 weeks after treatments. An orthogonal line is a linear regression line with $R^2 = 0.785$ ($p < 0.0001$). 2W, 2 weeks after treatment; 4W, 4 weeks after treatment; error bar, standard error of mean.

in the WT AB, KO AB, WT MB, and KO MB groups were 430.1 ± 14.7, 425.4 ± 14.5, 568.6 ± 18.2, and 565.2 ± 38.8 mm Hg-day, respectively, indicating that the WT MB and KO MB mice were 32.2% and 32.8% higher than AB counterparts, respectively (one-way ANOVA, $p < 0.001$; Tukey-Kramer, $p < 0.05$).

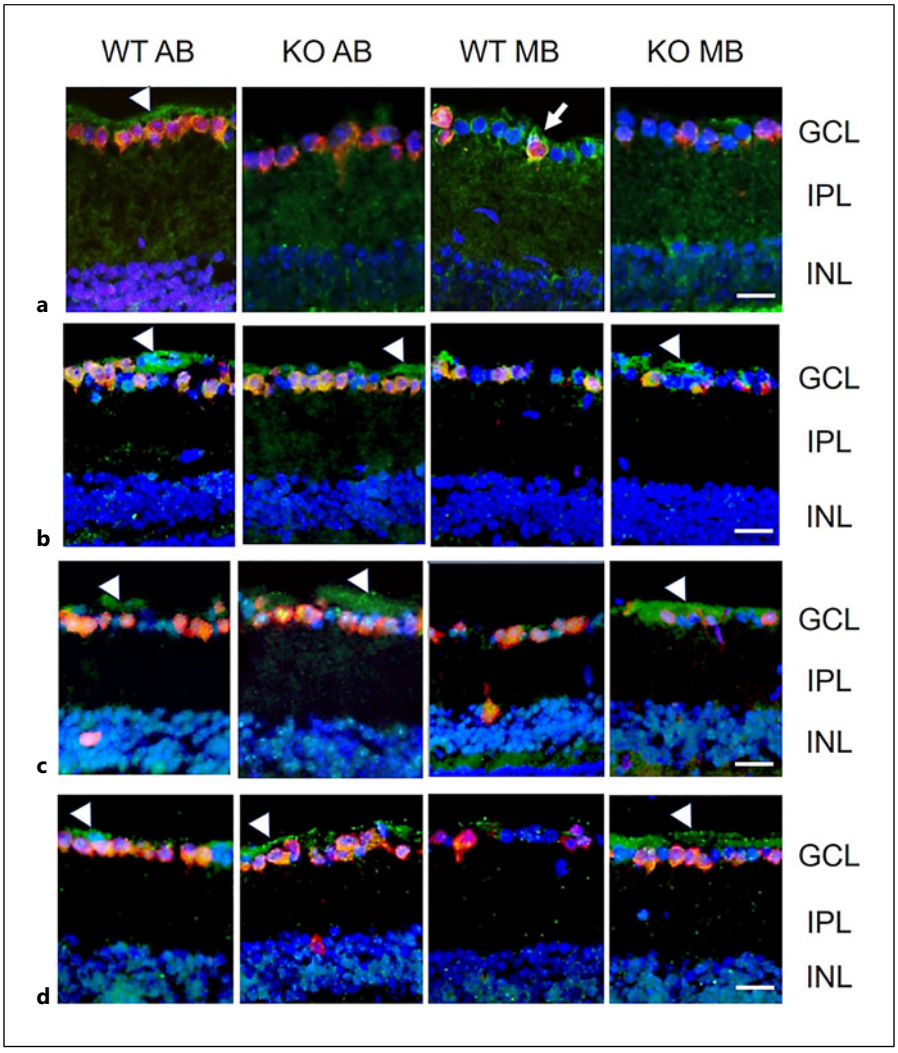

Fig. 3. Co-immuno-labeling of AQP9, MCT1, MCT2, and MCT4 (green) with RBPMS (red) in the inner retina of 4 groups of mice at 4 weeks after treatment. DAPI nuclear staining (blue) was also conducted. **a** AQP9 immunolabeling. **b** MCT1 immunolabeling. **c** MCT2 immunolabeling. **d** MCT4 immunolabeling. Scale bar, 25 μm. Arrowheads indicate immunoreactivity of AQP9, MCT1, MCT2, and MCT4 which is not co-labeled with RBPMS. An arrow indicates a representative RGC expressing both RBPMS and AQP9. GCL, ganglion cell layer; IPL, inner plexiform layer; INL, inner nuclear layer.

Effect of Elevated IOP on RGC Density

There was no difference in RGC density between WT and *Aqp9* KO mice at any time points, irrespective of MB or AB injection. The density significantly decreased at 2 and 4 weeks than at baseline in both WT and *Aqp9* KO mice (one-way ANOVA, $p < 0.001$; Tukey-Kramer test, $p < 0.05$) as shown in Figure 2a and b.

There was a significant correlation between cumulative IOP and RGC density at 4 weeks of treatment (Fig. 2c), with a R^2 of 0.785 ($p < 0.0001$). WT and KO mice show similar cumulative IOP and RGC cell density distributions after AB or MB injections.

Retinal Expression of AQP9 and MCT1, MCT2, and MCT4

Figure 3 demonstrates representative images of immunostaining of AQP9, MCT1, MCT2, and MCT4 (green), which were co-labeled with a RGC marker, RNA-binding protein with multiple splicing (RBPMS; red), and DAPI nuclear staining (blue). As shown in Figure 3, the WT AB mouse shows immunoreactivity for AQP9, MCT1, MCT2, and MCT4 not only in a portion of RBPMS-positive cells, as shown in yellow, but also in more superficial retinal layer (arrowheads). Considering their linear pattern of immunoreactivity, their superficial immunoreactivity is deemed to reflect astrocyte expression of these transporters. The KO AB mouse almost lost ganglion cell layer (GCL) AQP9 immunoreactivity, while MCT1 and MCT4 immunoreactivity were very similar to WT counterparts. Conversely, the GCL MCT2 immunoreactivity was enhanced compared to the WT. The WT MB mouse still showed AQP9 immunoreactivity surrounding the remaining RBPMS-positive cells (arrow), but lost the superficial linear pattern of AQP9 immunoreactivity at the GCL. MCT1 immunoreactivity was substantially reduced in these mice, but the reduction of MCT2 and MCT4 immunoreactivity was modest compared

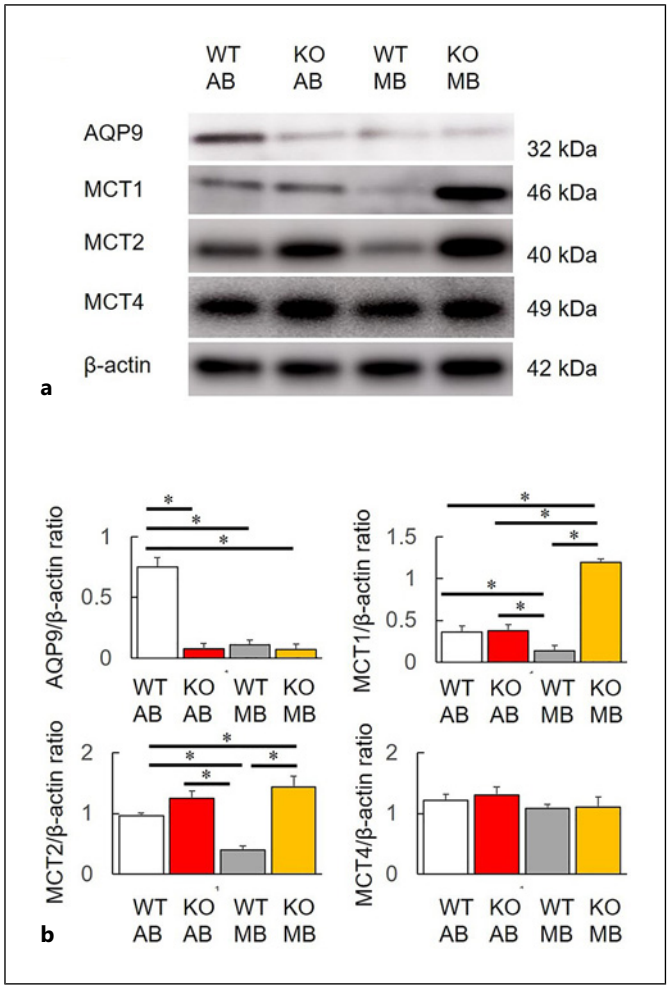

Fig. 4. Immunoblot analysis data of mouse retinas 4 weeks after treatment. **a** Representative blot images. **b** Data quantification expressed by relative ratio to β-actin expression. n = 4 per group. *ANOVA, $p < 0.001$; Tukey-Kramer test $p < 0.05$.

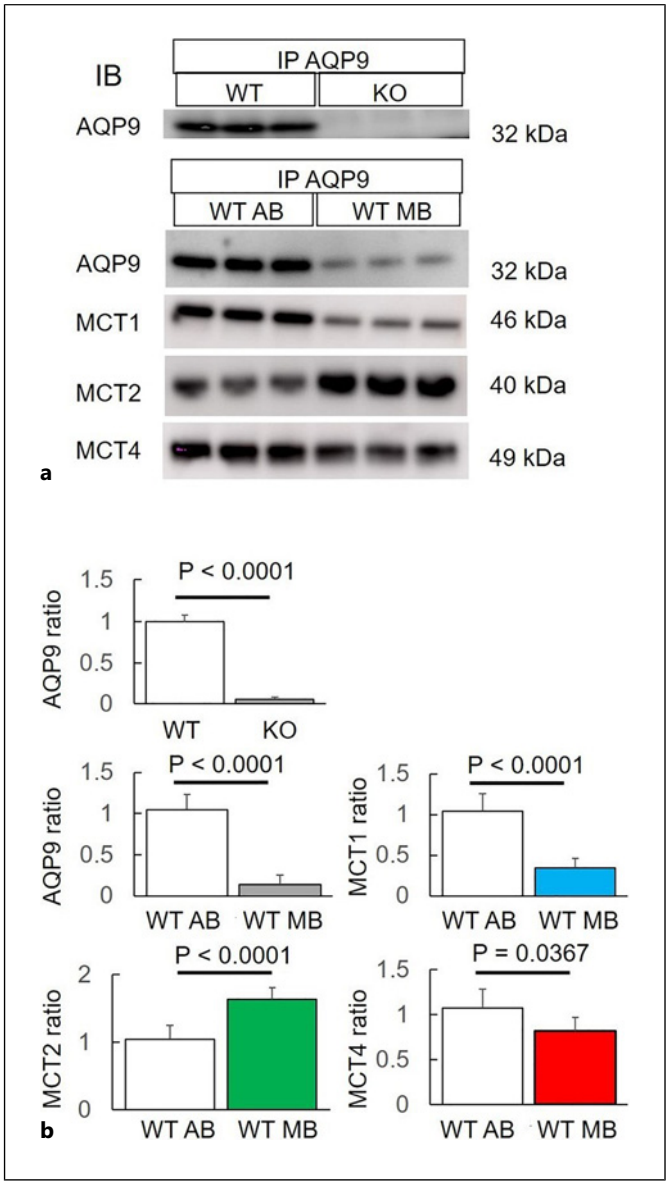

Fig. 5. Immunoblot for immunoprecipitation with AQP9 in mouse retinas 4 weeks after treatment. **a** Representative blot images. **b** Data quantification expressed by relative ratio to the average expression in WT mice. n = 3 per group. IP, immunoprecipitation; IB, immunoblot.

to the WT AB group. In contrast, the KO MB mouse showed no AQP9 immunoreactivity. Immunoreactivity for MCT1 and MCT4 was not much different from the KO AB mouse, while MCT2 immunoreactivity was rather enhanced.

Figure 4 shows immunoblot analysis data of mouse retina 4 weeks after treatment. Compared to the WT AB group, the remaining three groups showed significantly decreased AQP9 relative to β-actin expression (one-way ANOVA, $p < 0.001$; Tukey-Kramer test, $p < 0.05$). There were no differences in baseline expressions of MCT1, MCT2, and MCT4 between the WT and KO AB mice. The WT MB mice exhibited significantly reduced MCT1 and MCT2 expression than the other three groups ($p < 0.001$), while the KO MB group had significantly higher MCT1 than the remaining three groups ($p < 0.05$) and had significantly higher MCT2 than the WT AB and MB groups ($p < 0.05$). In contrast, MCT4 expression did not differ among the four groups ($p = 0.17$).

Interaction of MCTs 1, 2, and 4 with AQP9 Expression in Retina

Figure 5 depicts immunoblots for AQP9, MCT1, MCT2, and MCT4 co-immunoprecipitated with AQP9 in mouse retinas 4 weeks after treatment. Retinal AQP9

immunoprecipitates from the WT AB mice unsurprisingly revealed abundant AQP9 expression, whereas those from the KO AB group lacked AQP9 immunogenicity ($p < 0.0001$). The WT MB mice exhibited reduced AQP9 and MCT1 co-immunoprecipitated with AQP9 compared to the WT AB mice ($p < 0.0001$). In comparison, co-immunoprecipitated MCT2 was significantly increased ($p < 0.0001$). Conversely, the WT MB mice showed marginal reduction of MCT4 immunogenicity in AQP9 immunoprecipitates compared to WT AB mice ($p = 0.037$).

Discussion

The degree of cumulative IOP elevation and the eventual RGC density reduction rate both occurred in the present study and were comparable with previously reported results [14–17]. The comparable RGC density in WT and *Aqp9* KO mice at baseline replicated our previous report [3], supporting that *Aqp9* gene deletion alone does not induce RGC death under physiological conditions. Given no difference in RGC density between *Aqp9* KO mice and WT littermates even at 4 weeks after MB injection, *Aqp9* gene deletion did not modify the RGC density reduction induced by ocular hypertension. This looked contradicted with our previous study using ONC that a 44.9% reduction after ONC in WT mice significantly increased to 60.1% in *Aqp9* KO mice [3]. This discrepancy may be because ocular hypertension is a milder load on the RGCs and the optic nerve than ONC, possibly enabling RGCs to compensate for the compromised metabolisms [19]. Ocular hypertension reduced retinal AQP9 expression and changed GCL AQP9 immunoreactive pattern in WT mice as in ONC [3], optic nerve transection [7] in rodents, and in human glaucomatous eyes [8].

The major difference between the present study and the previous one using ONC [3] is the change in MCT expression in *Aqp9* KO mice. The MCT1 and MCT2 expression during ONC significantly increased in *Aqp9* KO mice compared to WT mice but did not exceed that of the sham group [3]. Meanwhile, ocular hypertension also increased both MCT protein expression in *Aqp9* KO mice, but the extent of the increase was significantly greater than in the KO AB mice. Additionally, ocular hypertension like ONC decreased MCT1 protein co-immunoprecipitated with AQP9, but the magnitude of the decrease was not as marked as in the case of ONC. Moreover, the MCT4 co-immunoprecipitated with AQP9 remained almost unchanged, while MCT2 counterparts rather increased, suggesting that MCT2 and MCT4 co-expressed with AQP9 were greatly enhanced by ocular hypertension stress, given overall AQP9 content reduction. These findings may indicate that elevated IOP not only alters AQP9, MCT2, and MCT4 individually but also impacts their protein-protein interaction. The mechanism by which high IOP enhances the interaction between AQP9 and MCT2 is unknown, but it is known that AQP9 has different isoforms [20, 21], and the AQP9 isoform that remains at elevated IOP may have higher affinity and binding ability with MCT2 than the AQP9 isoform whose expression decreases. Further studies should be warranted.

Conversely, conventional immunoblots revealed that MCT1 expression was greatly enhanced in KO MB mice, suggesting MCT1 independently expressed from AQP9 increased in these mice. Harun-Or-Rashid et al. [15] reported that MCT1, MCT2, and MCT4 expressions in the optic nerve are reduced in DBA/2J mice with spontaneous glaucoma and glaucoma mice with MB injection-induced elevated IOP. The following study by the same group revealed that MCT2 overexpression has neuroprotective effects on the retina and optic nerve [22]. Thus, the neuronal MCT2 among MCT family may play a fundamental role in RGC survival in the metabolically compromised retina in the context of ANLS [23–25].

The present study has limitations. First, there is no direct evidence for an affinity between MCTs and AQP9 despite a physical interaction between them. Second, the RGC has not been functionally evaluated. In conclusion, despite similar eventual RGC density reduction between the WT and *Aqp9* KO mice, ocular hypertension decreased the AQP9 and MCT1 and MCT2 expressions in GCL and MCT1-AQP9 interaction in the WT mice, while MCT1 and MCT2 expressions were rather enhanced in the *Aqp9* KO mice, possibly as a compensatory mechanism to maintain ANLS in the inner retina.

Acknowledgment

The authors thank AJE (https://www.aje.com/) for the English language review.

Statement of Ethics

Animal experiments were approved by the Animal Care Committee of the Kobe University Graduate School of Medicine (No. P200708) and conducted in accordance with the guidelines

stipulated in the Association for Research in Vision and Ophthalmology resolution on the care and use of laboratory animals.

Conflict of Interest Statement

The authors have no conflicts of interest to declare.

Funding Sources

This study was supported in part by Grants-in-Aid No. 21K09675 from the Japan Society for the Promotion of Science (Makoto Nakamura).

Author Contributions

Yusuke Murai conducted experiments, analyzed the data, and compiled the manuscript; Sotaro Mori and Sentaro Kusuhara interpreted the data and revised the manuscript; Mina Okuda was responsible for animal care and eye tissue processing and revised the manuscript; Takuji Kurimoto conducted experiments, analyzed the data, and revised the manuscript; and Makoto Nakamura designed the study, interpreted the data, and compiled the manuscript. All authors discussed the results and commented on the manuscript.

Data Availability Statement

All data generated or analyzed during this study are included in this article. Further inquiries can be directed to the corresponding author.

References

1 Jonas JB, Aung T, Bourne RR, Bron AM, Ritch R, Panda-Jonas S. Glaucoma. Lancet. 2017 Nov;390(10108):2183–93.
2 Magistretti PJ, Allaman I. Lactate in the brain: from metabolic end-product to signalling molecule. Nat Rev Neurosci. 2018 Apr;19(4):235–49.
3 Mori S, Kurimoto T, Miki A, Maeda H, Kusuhara S, Nakamura M. *Aqp9* gene deletion enhances retinal ganglion cell (RGC) death and dysfunction induced by optic nerve crush: evidence that aquaporin 9 acts as an astrocyte-to-neuron lactate shuttle in concert with monocarboxylate transporters to support RGC function and survival. Mol Neurobiol. 2020 Nov;57(11):4530–48.
4 Badaut J, Lasbennes F, Magistretti PJ, Regli L. Aquaporins in brain: distribution, physiology, and pathophysiology. J Cereb Blood Flow Metab. 2002 Apr;22(4):367–78.
5 Iandiev I, Pannicke T, Biedermann B, Wiedemann P, Reichenbach A, Bringmann A. Ischemia-reperfusion alters the immunolocalization of glial aquaporins in rat retina. Neurosci Lett. 2006 Nov;408(2):108–12.
6 Naka M, Kanamori A, Negi A, Nakamura M. Reduced expression of aquaporin-9 in rat optic nerve head and retina following elevated intraocular pressure. Invest Ophthalmol Vis Sci. 2010 Sep;51(9):4618–26.
7 Miki A, Kanamori A, Negi A, Naka M, Nakamura M. Loss of aquaporin 9 expression adversely affects the survival of retinal ganglion cells. Am J Pathol. 2013 May;182(5):1727–39.
8 Tran TL, Bek T, la Cour M, Nielsen S, Prause JU, Hamann S, et al. Altered aquaporin expression in glaucoma eyes. APMIS. 2014 Sep;122(9):772–80.
9 Akashi A, Miki A, Kanamori A, Nakamura M. Aquaporin 9 expression is required for l-lactate to maintain retinal neuronal survival. Neurosci Lett. 2015 Mar;589:185–90.
10 Barros LF, Deitmer JW. Glucose and lactate supply to the synapse. Brain Res Rev. 2010 May;63(1–2):149–59.
11 Riske L, Thomas RK, Baker GB, Dursun SM. Lactate in the brain: an update on its relevance to brain energy, neurons, glia and panic disorder. Ther Adv Psychopharmacol. 2017 Feb;7(2):85–9.
12 Rojek AM, Skowronski MT, Fuchtbauer EM, Fuchtbauer AC, Fenton RA, Agre P, et al. Defective glycerol metabolism in aquaporin 9 (AQP9) knockout mice. Proc Natl Acad Sci U S A. 2007 Feb;104(9):3609–14.
13 Mylonakou MN, Petersen PH, Rinvik E, Rojek A, Valdimarsdottir E, Zelenin S, et al. Analysis of mice with targeted deletion of AQP9 gene provides conclusive evidence for expression of AQP9 in neurons. J Neurosci Res. 2009 May;87(6):1310–22.
14 Ito YA, Belforte N, Cueva Vargas JL, Di Polo A. A Magnetic microbead occlusion model to induce ocular hypertension-dependent glaucoma in mice. J Vis Exp. 2016 Mar;109:e53731.
15 Harun-Or-Rashid M, Pappenhagen N, Palmer PG, Smith MA, Gevorgyan V, Wilson GN, et al. Structural and functional rescue of chronic metabolically stressed optic nerves through respiration. J Neurosci. 2018 May;38(22):5122–39.
16 Claes M, Moons L. Retinal ganglion cells: global number, density and vulnerability to glaucomatous injury in common laboratory mice. Cells. 2022 Aug;11(17):2689.
17 Yang Q, Cho KS, Chen H, Yu D, Wang W-H, Luo G, et al. Microbead-induced ocular hypertensive mouse model for screening and testing of aqueous production suppressants for glaucoma. Invest Ophthalmol Vis Sci. 2012 Jun;53(7):3733–41.
18 Gundersen HJ, Jensen EB, Kieu K, Nielsen J. The efficiency of systematic sampling in stereology—reconsidered. J Microsc. 1999 Mar;193(Pt 3):199–211.
19 Calkins DJ. Adaptive responses to neurodegenerative stress in glaucoma. Prog Retin Eye Res. 2021 Sep;84:100953.
20 Amiry-Moghaddam M, Lindland H, Zelenin S, Roberg BA, Gundersen BB, Petersen P, et al. Brain mitochondria contain aquaporin water channels: evidence for the expression of a short AQP9 isoform in the inner mitochondrial membrane. FASEB J. 2005 Sep;19(11):1459–67.
21 Opdal SH, Ferrante L, Rognum TO, Stray-Pedersen A. Aquaporin-1 and aquaporin-9 gene variations in sudden infant death syndrome. Int J Legal Med. 2021 May;135(3):719–25.
22 Harun-Or-Rashid M, Pappenhagen N, Zubricky R, Coughlin L, Jassim AH, Inman DM. MCT2 overexpression rescues metabolic vulnerability and protects retinal ganglion cells in two models of glaucoma. Neurobiol Dis. 2020 Jul;141:104944.
23 Smith D, Pernet A, Hallett W, Bingham E, Marsden PK, Amiel SA. Lactate: a preferred fuel for human brain metabolism in vivo. J Cereb Blood Flow Metab. 2003 Jun;23(6):658–64.
24 Baltan S. Can lactate serve as an energy substrate for axons in good times and in bad, in sickness and in health? Metab Brain Dis. 2015 Feb;30(1):25–30.
25 Vohra R, Kolko M. Lactate: more than merely a metabolic waste product in the inner retina. Mol Neurobiol. 2020 Apr;57(4):2021–37.